EUROPHYSICS LETTERS 15 July 2005

Europhys. Lett., **71** (2), pp. 159–165 (2005)
DOI: 10.1209/epl/i2005-10085-3

Motion of vortices implies chaos in Bohmian mechanics

D. A. Wisniacki[1] and E. R. Pujals[2,3]

[1] *Departamento de Física "J. J. Giambiagi", FCEN, UBA - Pabellón 1 Ciudad Universitaria, 1428 Buenos Aires, Argentina*
[2] *Department of Mathematics, University of Toronto Toronto, Ontario, Canada M5S 3G3*
[3] *IMPA-OS - Dona Castorina 110, 22460-320 Rio de Janeiro, Brazil*

received 21 March 2005; accepted in final form 25 May 2005
published online 17 June 2005

PACS. 03.65.-w – Quantum mechanics.
PACS. 03.65.Ta – Foundations of quantum mechanics; measurement theory.

Abstract. – Bohmian mechanics is a causal interpretation of quantum mechanics in which particles describe trajectories guided by the wave function. The dynamics in the vicinity of nodes of the wave function, usually called vortices, is regular if they are at rest. However, vortices generically move during time evolution of the system. We show that this movement is the origin of chaotic behavior of quantum trajectories. As an example, our general result is illustrated numerically in the two-dimensional isotropic harmonic oscillator.

De Broglie-Bohm's (BB) approach to quantum mechanics has experienced an increased popularity in recent years. This is due to the fact that it combines the accuracy of the standard quantum description with the intuitive insight derived from the causal trajectory formalism, thus providing a powerful theoretical tool to understand the physical mechanisms underlying microscopic phenomena [1, 2]. Although the behavior of quantum trajectories is very different from classical solutions, it can be used to gain intuition in many physical phenomena. Numerous examples can be found in different areas of research. In particular, we can mention studies of barrier tunneling in smooth potentials [3], the quantum back-reaction problem [4] and ballistic transport of electrons in nanowires [5].

According to the BB theory of quantum motion, a particle moves in a deterministic orbit under the influence of the external potential and a quantum potential generated by the wave function. This quantum potential can be very intricate because it encodes information on wave interferences. Based on it, Bohm already predicted complex behavior of the quantum trajectories in his seminal work [6]. This was recently confirmed in several studies when the presence of chaos in various systems has been shown numerically [7–9]. However, the mechanisms that cause such a complex behavior is still lacking. In this letter we show that movement of the zeros of the wave function, commonly known as vortices, implies chaos in the dynamics of quantum trajectories. Such a movement perturbs the velocity field producing transverse homoclinic orbits that generate the well-known Smale horseshoes which is the origin of complex behavior. Our assertion is based on an analytical proof in a simplified model which resembled the velocity field near the vortices. In addition, we present a numerical study in a

© EDP Sciences
Article published by EDP Sciences and available at http://www.edpsciences.org/epl or http://dx.doi.org/10.1209/epl/i2005-10085-3

2D isotropic harmonic oscillator that displays a route to chaos dominated by this mechanism. It is important to mention that there is no agreement in previous works about the influence of vortices on the chaotic motion of quantum trajectories [8–11].

The fundamental equations in the BB theory are derived from the introduction of the wave function in polar form, $\psi(\boldsymbol{r},t)=R(\boldsymbol{r},t)\,\mathrm{e}^{\mathrm{i}S(\boldsymbol{r},t)}$ (throughout the paper $\hbar$ is set equal to 1), into the time-dependent Schrödinger equation, thus obtaining two real equations:

$$\frac{\partial R^2}{\partial t}+\nabla\cdot\left(R^2\,\frac{\nabla S}{m}\right)=0, \tag{1}$$

$$\frac{\partial S}{\partial t}+\frac{(\nabla S)^2}{2m}+V-\frac{1}{2m}\frac{\nabla^2 R}{R}=0, \tag{2}$$

which are the continuity and quantum Hamilton-Jacobi equations, respectively. The last term in the left-hand side of eq. (2) is the so-called quantum potential, a non-local function determined by the quantum state, which, together with V, determines the total force acting on the system. Similarly to what happens in the usual classical Hamilton-Jacobi theory, quantum trajectories of a particle of mass m can then be defined by means of the following velocity field equation:

$$\boldsymbol{v}=\dot{\boldsymbol{r}}=\frac{1}{m}\nabla S=\frac{i}{2m}\frac{\psi\nabla\psi^*-\psi^*\nabla\psi}{|\psi|^2}\,. \tag{3}$$

Vortices appear naturally in the BB framework. They result from wave function interferences so they have no classical explanation. In systems without magnetic field, the *bulk* vorticity $\nabla\times\boldsymbol{v}$ in the probability fluid is determined by the points where the phase S is singular. This may occur only at points where the wave function vanishes. This condition is fulfilled by isolated points in a 2D system and lines in a 3D system. Due to the single-valuedness of the wave function, the circulation Γ along any closed contour ξ encircling a vortex must be quantized, that is

$$\Gamma=\int_\xi \dot{\boldsymbol{r}}\,\mathrm{d}\boldsymbol{r}=\frac{2\pi n}{m}\,, \tag{4}$$

with n an integer [12,13]. So, the velocity $\boldsymbol{v}$ must diverge as one approaches a vortex. In fact, the time-dependent velocity field in the vicinity of a vortex located at time t in $\boldsymbol{r}_{\boldsymbol{v}}(t)$ is given by

$$\boldsymbol{v}=\frac{-i}{2m}\frac{[\boldsymbol{r}-\boldsymbol{r}_{\boldsymbol{v}}(t)]\times\boldsymbol{w}\times\boldsymbol{w}^*}{|[\boldsymbol{r}-\boldsymbol{r}_{\boldsymbol{v}}(t)]\cdot\boldsymbol{w}|^2}\,, \tag{5}$$

where $\boldsymbol{w}\equiv\nabla\psi(\boldsymbol{r}_{\boldsymbol{v}}(t))$ [10,14]. We consider here 2D systems but we believe that our results are valid for systems of higher dimensions.

Before presenting our analytical results, we show a numerical simulation of quantum trajectories in a system consisting of a particle of unit mass in a 2D isotropic harmonic oscillator. We have set the angular frequency $\omega=1$, so the Hamiltonian of the system results to be

$$H=-\frac{1}{2}\left(\frac{\partial^2}{\partial x^2}+\frac{\partial^2}{\partial y^2}\right)+\frac{1}{2}\big(x^2+y^2\big). \tag{6}$$

The eigenenergies are $E_{n_xn_y}=n_x+n_y+1$ and the eigenfunctions $\phi_{n_xn_y}(x,y)=\exp[-\frac{1}{2}(x^2+y^2)]H_{n_x}(x)H_{n_y}(y)/\sqrt{\pi\;2^{n_x+n_y}\;n_x!\;n_y!}$ with $n_x=0,1,\ldots$, $n_y=0,1,\ldots$, where H_n is the n-th–degree Hermite polynomial.

We have chosen the following general combination of the first three eigenstates of the Hamiltonian of eq. (6) as initial state:

$$\psi_0=a\phi_{00}+b\exp[-i\gamma_1]\phi_{10}+c\exp[-i\gamma_2]\phi_{01}\,, \tag{7}$$

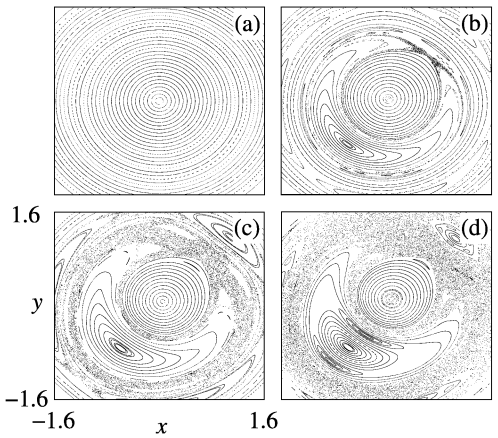

Fig. 1

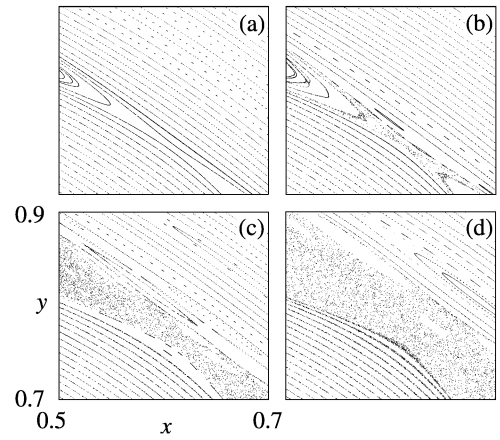

Fig. 2

Fig. 1 – Poincaré surface of section for the quantum trajectories generated by the wave function of eq. (7) with $b = c$ and $a/b = 0$ (a), 0.0553 (b), 0.1138 (c) and 0.17651 (d) with fixed value of $\gamma_1 = 3.876968$ and $\gamma_2 = 2.684916$. The trajectories of the vortex of the corresponding wave functions are shown in fig. 3.

Fig. 2 – Part of the Poincaré surface of section for the quantum trajectories generated by the wave function of eq. (7) with small values of a/b. The parameter $b = c$ and $a/b = 0.01082$ (a), 0.02175 (b), 0.0328 (c) and 0.0440 (d) with fixed value of $\gamma_1 = 3.876968$ and $\gamma_2 = 2.684916$.

with a, b, c, γ_1 and γ_2 real numbers and $a^2 + b^2 + c^2 = 1$ (the normalization condition). A remarkable point is that this state generates a periodic time-dependent velocity field with only one vortex. Moreover, the trajectory of the vortex can be obtained analytically resulting:

$$\boldsymbol{r_v}(t) = (x_v(t), y_v(t)) = \left(\frac{a}{\sqrt{2}b} \frac{\sin(\gamma_2 - t)}{\sin(\gamma_1 - \gamma_2)}, \frac{a}{\sqrt{2}c} \frac{\sin(\gamma_1 - t)}{\sin(\gamma_1 - \gamma_2)} \right). \tag{8}$$

This fact allows us to see the influence of the movement of a vortex in the dynamics of the quantum trajectories, without taking into account the possibility of instantaneous creation or annihilation of a vortex pair with opposite circulation [14, 15]. This important phenomenon will be studied elsewhere [16].

The non-autonomous velocity field generated by the wave function of eq. (7) is periodic so the best surface of section is given by fixing $t = 2\pi n$ with $n = 0, 1, \ldots$ (also called a stroboscopic view). Figure 1 shows surfaces of section with $b = c$ and $a/b = 0, 0.0553, 0.1138$ and 0.17651 with fixed value of $\gamma_1 = 3.876968$ and $\gamma_2 = 2.684916$. A clear transition to chaos appears as the parameter a/b is increased. If the position of the vortex is fixed, the trajectories are regular and no chaos is present (see fig. 1(a)). However, irregular dynamics is observed for small a/b (fig. 1(b)). The transition to irregular dynamics is shown in fig. 2. The movement of the vortex produces a saddle point near $(0.6, 0.75)$ and its stable and unstable manifolds have a topological transverse intersection generating the well-known homoclinic tangle [17]. The trajectories of the vortex for the cases studied in fig. 1 are plotted in fig. 3.

Now we will show analytical results that explain the numerical experiments presented before. Our starting point is the following model: a particle of unit mass on the plane in the velocity field of eq. (5) with the constraints that the trajectory of the vortex is a time-periodic

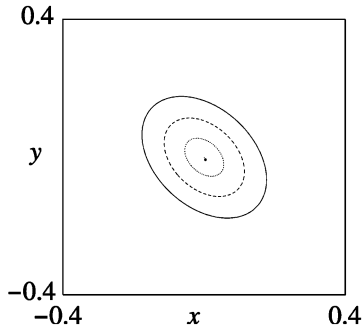

Fig. 3 – Path described by the vortex (eq. (8)) of the velocity field generated by wave functions of eq. (7) with $b = c$ and $a/b = 0$ (filled circle), 0.0553 (dotted line), 0.1138 (dashed line) and 0.17651 (solid line) with fixed value of $\gamma_1 = 3.876968$ and $\gamma_2 = 2.684916$.

curve and $w_x = iw_y$ [18]. Thus, the non-autonomous vector field is equal to

$$\begin{aligned} v_x &= \frac{-(y - y_v(t))}{(x - x_v(t))^2 + (y - y_v(t))^2}, \\ v_y &= \frac{(x - x_v(t))}{(x - x_v(t))^2 + (y - y_y(t))^2}. \end{aligned} \tag{9}$$

Taking $\bar{x} = x - x_v(t)\, \bar{y} = y - y_v(t)$ and writing in polar coordinates ($\bar{x} = r\cos(\theta)$, $\bar{y} = r\sin(\theta)$), the velocity field of eq. (9) results:

$$\begin{aligned} v_r &= r[\sin(\theta)y_v(t) + x_v(t)\cos(\theta)], \\ v_\theta &= \frac{1}{r} + \cos(\theta)y_v(t) - x_v(t)\sin(\theta). \end{aligned}$$

This non-autonomous velocity field can be seen as a perturbation of the autonomous velocity field $\boldsymbol{v}_0 \equiv (0, \frac{1}{r})$, with $\boldsymbol{G}(r, \theta, t) \equiv (r[\sin(\theta)y_v(t) + x_v(t)\cos(\theta)], \cos(\theta)y_v(t) - x_v(t)\sin(\theta))$ the time-periodic perturbation. Note that the field is induced by the time-dependent Hamiltonian

$$H(r, \theta, t) = \frac{1}{2}\log(r) + r[\cos(\theta)y_v(t) - \sin(\theta)x_v(t)]. \tag{10}$$

We consider periodic curves $\boldsymbol{r_v}(t)$ such that

$$\int_0^{T_0} \cos(\theta)y_v(t) - x_v(t)\sin(\theta)\mathrm{d}t\, \mathrm{d}s \neq 0. \tag{11}$$

Under these hypothesis the following property can be proved:

There exists a saddle periodic orbit of the flow associated to the vector field of eq. (9), exhibiting a homoclinic transversal intersection.

This result, which implies that quantum trajectories show topological chaos, is the main finding of our work. We illustrate here the geometrical arguments of the proof and we leave the full details for a future publication [19]. We notice that a periodic orbit of saddle type exhibits a homoclinic transversal intersection if its stable and unstable manifolds intersect each other and the tangents of the manifolds are not collinear at the intersection. Transversal homoclinic intersections (or homoclinic tangles) beat at the heart of chaos. This is because

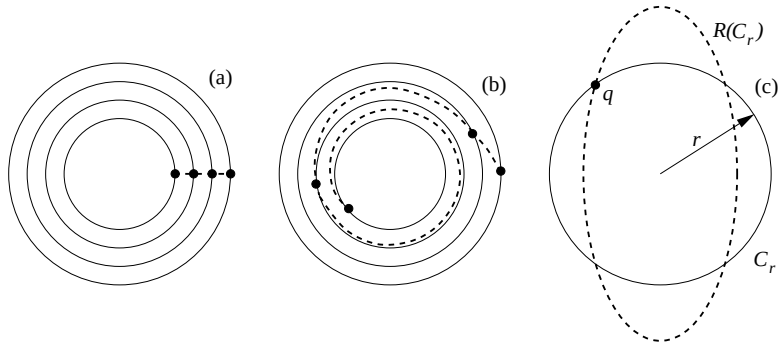

Fig. 4 – (a) Schematic plot of the invariants of the non-perturbed map R^0 generated by the autonomous velocity field $\boldsymbol{v}_0$ (solid lines). With dashed line it is plotted a segment with $\theta = 0$. (b) Non-perturbed mapped R^0 of the segment with $\theta = 0$ (dashed line). (c) It is showed with dashed line the image of the perturbed map R of a circle C_r with radius r (solid line). A point $q \in R(C_r) \cap C_r$ is also plotted.

in the region of a homoclinic tangle, initial conditions are subject to a violent stretching and folding process, the two essential ingredients for chaotic behavior.

Let us start to show the main result of the letter considering some important charateristics and properties of the flows generated by the velocity fields $\boldsymbol{v}_0$ and $\boldsymbol{v}$. The flow Φ_t^0 associated with the autonomous velocity field $\boldsymbol{v}_0$ is defined for every $(\bar{x}, \bar{y}) \neq (0,0)$. Thus, given a positive time T_0, the map $R^0 = \Phi_{T_0}^0 : \Re^2 \setminus \{(0,0)\} \to \Re^2 \setminus \{(0,0)\}$ is well defined. It is straightforward to show that the map R^0 written in polar coordinates results to be $R^0 = (R_r^0(r,\theta), R_\theta^0(r,\theta)) = (r, \theta + \frac{1}{r}T_0)$. Map R^0 keeps invariant the set of points with same radius; *i.e.*, it keeps invariant the circles. Moreover, the circles are rotated with a rate of rotation inversely proportional to the radius (see fig. 4(a) and (b)). Observe that map R^0 resembles a twist map with the difference that in the present case, the rate of rotation grows to infinity when the radius is reduced. In this respect, it is important to mention that for generic conservative perturbations of the twist map the existence of homoclinic points associated to a saddle periodic point was proved [20]. This result was also extended to time-periodic perturbations of a flow which exhibit an elliptic singularity [21].

We have assumed that the vortex moves periodically along a curve, that is, $\boldsymbol{r_v}(t) = \boldsymbol{r_v}(t + T_0)$. Then, the time-dependent velocity field $\boldsymbol{v}$ induces a flow Φ_t which is defined for every $(\bar{x}, \bar{y}) \neq \{(0,0)\}$. So, the map $R = \Phi_{T_0} : \Re^2 \setminus \{(0,0)\} \to \Re^2 \setminus \{(0,0)\}$ is well defined. Note that flow Φ_t is generated by a time-periodic Hamiltonian (eq. (10)), so R is a conservative map. Also, R can be extended continuously to $(0,0)$ defining $R(0,0) \equiv (0,0)$ (note that $R \to 0$ when $(\bar{x}, \bar{y}) \to (0,0)$). Then, it follows that map R verifies:

Property A: Like R^0, map R also has the property that circles are rotated with a rate of rotation inversely proportional to the radius (see fig. 4(a) and (b)). In other words, if map R is written in polar coordinates $R(r,\theta) = (R_r(r,\theta), R_\theta(r,\theta))$, then $\partial_r R_\theta$ is of the order of $1/r^2$.

Property B: The image of a small circle of radius r intersects transversally this circle; *i.e.* $R(C_r) \cap C_r \neq \emptyset$ and if $q \in R(C_r) \cap C_r$ then the tangent to $R(C_r)$ and to C_r in q are not collinear (see fig. 4(c)).

From *properties A* and *B* of the perturbed map R it follows that for arbitrarily small r the map R has a fixed point p_0 with radius smaller than r exhibiting homoclinic transversal point. Of course, this result implies that the vector field of eq. (9) has a saddle periodic orbit with an homoclinic transversal intersection.

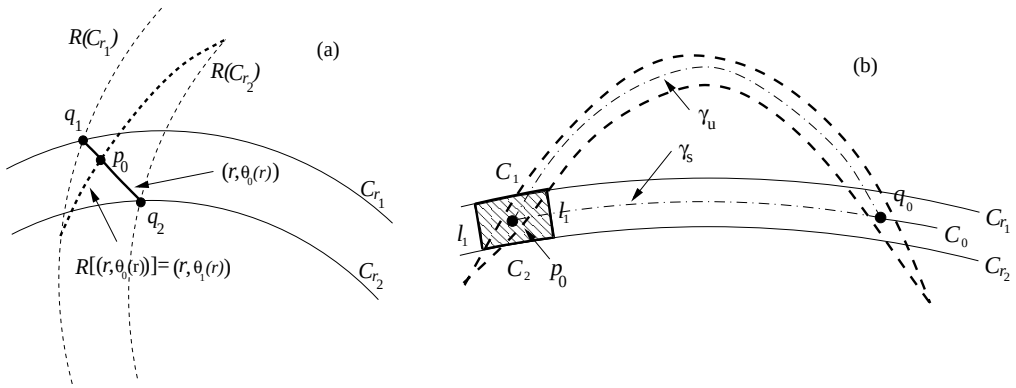

Fig. 5 – Schematic plots to show the existence of a saddle periodic point p_0 of the map R with a homoclinic transversal intersection. (a) The curve $r \to (r, \theta_0(r))$ is plotted with a thick solid line, and the curve $r \to R((r, \theta_0(r))) = (r, \theta_1(r))$ is plotted with a thick dashed line. Two invariants circles (C_{r_1} and C_{r_2}) and their perturbed mapping are also plotted. Note the transversal intersection between the circles an their respective mapping (points q_1 and q_2). (b) The rectangle B (hatched area) is bounded by two pieces of arcs C_1 and C_2 contained in C_{r_1} and C_{r_2} (where r_1 and r_2 are closed to r_0 verifying $r_1 < r_0 < r_2$) and two segments l_1 and l_2 contained in two different rays of constant angle. The segments γ_u and γ_s, that connect the periodic point p_0 with the transversal intersection q_0, are plotted with dash-dotted lines. The mapping $R(B)$ of the considered rectangle is also plotted with a thick dashed line.

We show the previous result in two steps. First, let us show that the perturbed map R has a fixed point. *Property B* guarantees the existence of the curve $(r, \theta_0(r))$ plotted in fig. 5(a). Note that $\theta_0(r)$ is the angular coordinate of a point on the intersection of a circle C_r with its image $R(C_r)$. A point on such a curve is mapped to another point with the same radius r but with a different angle $\theta_1(r)$,

$$R(r, \theta_0(r)) = (R_r(r, \theta_0(r)), R_\theta(r, \theta_0(r))) = (r, \theta_1(r)).$$

It is clear that map R has a fixed point if there exists an r_0 such that $\theta_0(r_0) = \theta_1(r_0)$. In other words, curves $(r, \theta_0(r))$ and $(r, \theta_1(r))$ of fig. 5(a) intersect at r_0. From *property A* it follows that the variation of $\theta_1(r)$ is larger than the variation of $\theta_0(r)$; in fact, the derivative of $\theta_1(r)$ is of the order of $1/r^2$. This fact guarantees the existence of r_0 in the vicinity of $r \to 0$ [19].

Now we will see that the mentioned fixed point has a transversal homoclinic intersection of its stable and unstable manifolds. We recall that the stable manifold is the set of points that converges to the fixed point by forward iteration of the dynamic. Conversely, the points on the unstable manifold converge to the fixed point by backward iteration. In fig. 5(b) we consider a circle C_0 of radius r_0 containing the fixed point p_0. Due to *property B*, C_0 and its image $R(C_0)$ have at least an additional point of intersection denoted by q_0. Points p_0 and q_0 are connected by the segments γ_s and γ_u of C_0 and $R(C_0)$, respectively. Let us consider the hatched rectangle B of fig. 5(b) that contains the fixed point p_0. Using *property A*, we have deduced that segments of constant angle l_1 and l_2 are stretched by R, and this shows that rectangle B is contracted by R along directions close to the tangent of the circles C_r and expanded along vectors close to the tangent of $R(C_r)$. This is displayed in fig. 5(b), where the mapping of the rectangle B is plotted with a thick dashed line. Moreover, we have proved in ref. [19] that $R(B)$ is close to γ_u and intersects C_0 in a point near q_0, and that $R^{-1}(B)$ is close to γ_s and intersects C_0 near q_0. This implies that the unstable manifold of p_0 is close to

γ_u and the stable manifold is close to γ_s. We recall that γ_u crosses γ_s at q_0, then the stable and unstable manifolds of p_0 have a transversal intersection near q_0.

In summary, we have found an universal mechanism leading to quantum trajectories having chaotic behavior. We have shown that the movement of vortices is a generic time-dependent perturbation of an autonomous velocity field which creates a saddle periodic orbit with a transversal homoclinic intersection of its stable and unstable manifolds. This transversal intersection generates the well-known Smale horseshoe which is the origin of complexity. Our results should be useful due to the fact that such deterministic quantum orbits are an important theoretical tool for understanding and interpreting several processes in different fields. On the other hand, our geometrical analysis of a singular velocity field could be important for both theoretical and applied problems of dynamical systems, as for example advection in non-stationary fluids [22].

* * *

This work received financial support from CONICET and UBACYT (X248). We thank G. Lozano and F. Duffy for useful comments.

REFERENCES

[1] Holland P. R., *The Quantum Theory of Motion* (Cambridge University Press, Cambridge) 1993.
[2] Dürr D., Goldstein S. and Zanghì N., *J. Stat. Phys.*, **67** (1992) 843.
[3] Lopreore C. L. and Wyatt R. E., *Phys. Rev. Lett.*, **82** (1999) 5190.
[4] Prezhdo O. V. and Brooksby C., *Phys. Rev. Lett.*, **86** (2001) 3215.
[5] Wu H. and Sprung D. W. L., *Phys. Lett. A*, **196** (1994) 229.
[6] Bohm D., *Phys. Rev.*, **85** (1952) 166; **85** (1952) 194.
[7] Parmenter R. H. and Valentine R. W., *Phys. Lett. A*, **201** (1995) 1; Konkel S. and Malowski A. J., *Phys. Lett. A*, **238** (1998) 95; Sales J. A. and Florencio J., *Phys. Rev. E*, **67** (2003) 016216.
[8] Frisk H., *Phys. Lett. A*, **227** (1997) 139.
[9] Wu H. and Sprung D. W. L., *Phys. Lett. A*, **261** (1999) 150.
[10] Falsaperla P. and Fonte G., *Phys. Lett. A*, **316** (2003) 382.
[11] Valentini A. and Westman H., *Proc. R. Soc. London, Ser. A*, **461** (2005) 253.
[12] Dirac P. A. M., *Proc. R. Soc. London, Ser. A*, **133** (1931) 60.
[13] Bialynicki-Birula I. and Bialynicki-Birula Z., *Phys. Rev. D*, **3** (1971) 2410.
[14] Bialynicki-Birula I., Bialynicki-Birula Z. and Sliwa C., *Phys. Rev. A*, **61** (2000) 5190.
[15] Hirschfelder J. O., *J. Chem. Phys.*, **67** (1978) 5477.
[16] Wisniacki D. A., Borondo F. and Pujals E., *Vortices and complexity in the quantum fluid*, in preparation.
[17] Palis J. and Takens F., *Hyperbolicity and Sensitive Chaotic Dynamics at Homoclinic Bifurcations* (Cambridge University Press, Cambridge) 1993.
[18] This is the simplest toy model because w_x and w_y are time-dependent functions given by the derivatives of the wave function.
[19] Pujals E. and Wisniacki D. A., in preparation.
[20] Zehnder E., *Comm. Pure Appl. Math.*, **26** (1973) 131.
[21] Guckenheimer J. and Holmes Ph., *Nonlinear Oscillations, Dynamical Systems, and Bifurcations of Vector Fields* (Springer-Verlag, New York) 1990.
[22] Kuznetsov L. and Zaslavsky G. M., *Phys. Rev. E*, **58** (1998) 7330; Boffeta G., Celani A. and Franzese P., *J. Phys. A*, **29** (1996) 3749.